

## Magnetic field resulting from nonlinear electrical transport in single crystals of charge-ordered $\text{Pr}_{0.63}\text{Ca}_{0.37}\text{MnO}_3$

Ayan Guha

*Department of Physics, Indian Institute of Science, Bangalore 560 012, India  
and CSIR Center of Excellence in Chemistry, Jawaharlal Nehru Center for Advanced Scientific Research, Jakkur P.O.,  
Bangalore 560 064, India*

N. Khare and A. K. Raychaudhuri

*National Physical Laboratory, Dr. K.S. Krishnan Marg, New Delhi 110012, India*

C. N. R. Rao

*CSIR Center of Excellence in Chemistry, Jawaharlal Nehru Center for Advanced Scientific Research, Jakkur P.O.,  
Bangalore 560 064, India*

(Received 8 May 2000)

In this paper we report that the current induced destabilization of the charge ordered (CO) state in a rare-earth manganite gives rise to regions with ferromagnetic correlation. We did this experiment by measuring the  $I$ - $V$  characteristics in single crystal of the CO system  $\text{Pr}_{0.63}\text{Ca}_{0.37}\text{MnO}_3$  and simultaneously measuring the magnetization of the current carrying conductor using a high  $T_c$  superconducting quantum interference device working at  $T=77$  K. We have found that the current induced destabilization of the CO state leads to a regime of negative differential resistance which leads to a small enhancement of the magnetization of the sample, indicating ferromagnetically aligned moments.

Electrical transport in rare-earth manganites has attracted considerable current interest because of a number of novel properties, like colossal magnetoresistance (CMR) and charge ordering (CO).<sup>1,2</sup> These manganites belong to the  $ABO_3$ -type perovskite oxides and have a general chemical formula of  $Re_{(1-x)}A_x\text{MnO}_3$ , where  $Re$  is the rare-earth element such as La, Nd, and Pr and  $A$  is an alkaline-earth element such as Ca, Sr, and Ba. These manganites, depending on the size of the average  $A$  site cationic radius, can charge order, in particular, when  $x = 1/2, 2/3, 4/5$ , etc. The formation of the CO state can also occur for other incommensurate values of the carrier concentration.

The CO state is strongly destabilized by different types of perturbations which include magnetic field,<sup>1</sup> electric field,<sup>3,4</sup> and optical radiation.<sup>5,6</sup> Application of an applied magnetic field of sufficient magnitude can lead to a collapse of the CO gap,  $\Delta_{CO}$ , at the Fermi level, and the melting of the charge-ordered insulating (COI) state to a ferromagnetic metallic (FMM) state.<sup>7,8</sup> Laser radiation creates conducting filaments which at low temperatures lead to nonlinear transport.<sup>5</sup> Application of an electric field beyond a threshold value also gives rise to nonlinear conduction accompanied by a broadband noise of substantial magnitude.<sup>9</sup> A topic of considerable current interest is what causes the destabilization of the CO state and whether the underlying mechanism is the same for all the perturbations.

An important issue associated with the formation of the COI state is that of spin ordering. For  $T > T_{CO}$  [i.e., in the paramagnetic (PM) phase], the dominant spin correlation is ferromagnetic (FM) which grows on cooling.<sup>10</sup> At  $T < T_{CO}$ , the FM spin correlations decrease till AFM ordering sets in at  $T_N$ . The COI state is generally stabilized by anti-

ferromagnetic (AFM) spin correlations. The metallic state, on the other hand, is stabilized by FM spin correlations. The presence of ferromagnetic interaction inhibits the formation of the COI state. In other words, the destabilization of the COI state by any interaction or external stimulus is expected to suppress AFM spin correlations and promote FM spin correlations. One can therefore surmise that when the COI state is destabilized, by whatever means, there should be a magnetic signature of the transition in terms of the enhanced magnetic moment.

In this paper, we have tested the above hypothesis in single crystals of charge-ordered  $\text{Pr}_{0.63}\text{Ca}_{0.37}\text{MnO}_3$  by simultaneous measurement of  $I$ - $V$  characteristics and detection of the magnetic moment by a high  $T_c$  superconducting quantum interference device (SQUID).

Single crystals of  $\text{Pr}_{0.63}\text{Ca}_{0.37}\text{MnO}_3$  were grown by a float zone technique in an image furnace. The crystal used for our experiment was cut to a size of  $4 \times 2 \times 0.3$  mm<sup>3</sup>, and current and voltage probes were attached to it with Ag-In alloy with a mean separation of the probes  $\approx 0.25$  mm. All the measurements were performed at  $T=77$  K by dipping the sample in a liquid nitrogen bath. The nonlinear  $I$ - $V$  characteristics were taken by biasing the sample with a constant current supply. The high  $T_c$  SQUID used<sup>11</sup> for the detection of the magnetic moment was based on BSCCO film operating at  $T \approx 77$  K which is capable of detecting a field weaker than  $10^{-10}$  T.

The schematic of the rf SQUID setup used to detect the small magnetic field associated with the destabilization of the COI state is shown in Fig. 1. The high  $T_c$  SQUID is based on a natural grain boundary junction in BScCO film ( $T_c \approx 108$  K) deposited on a single crystal SrTiO<sub>3</sub> substrate

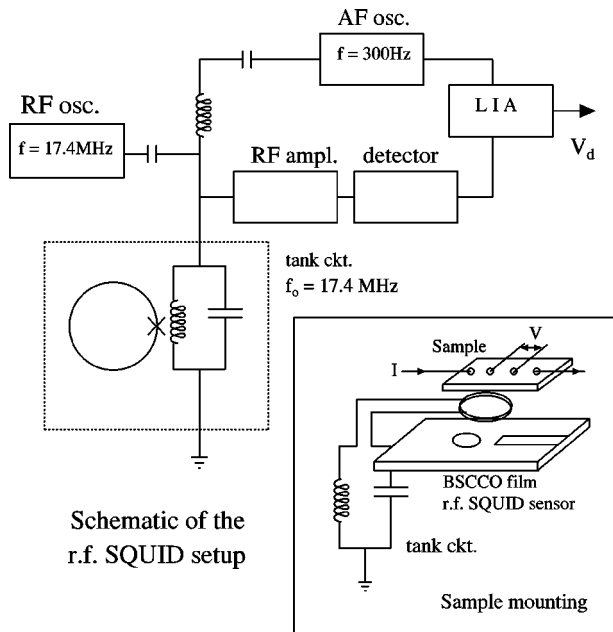


FIG. 1. Schematic of the high  $T_c$  rf SQUID setup (working at  $T=77$  K) employed for measuring small changes in magnetization in the current carrying sample. Also shown is the sample mounting arrangement.

by a screen printing technique. The SQUID geometry consists of a hole of diameter  $300 \mu\text{m}$  and a microbridge of width  $80 \mu\text{m}$ . rf biasing of the SQUID is applied through a tank circuit whose resonance frequency and quality factor ( $Q$ ) are  $17.5 \text{ MHz}$  and  $50$ , respectively. The inductance of the tank circuit consists of three coils of diameter approximately  $1 \text{ mm}$ : two of  $25$  turns ( $\# 38 \text{ SWG}$  copper) and one of  $8$  turns. The  $8$  turn coil is mounted concentrically on the hole on the surface of the BSCCO film. Three concentric cylinders of  $\mu$  metal are used to shield the SQUID and the sample from the external magnetic field. The tank circuit was driven at  $V_{rf} \approx 750 \mu\text{V}$ . Phase sensitive detection using a lock-in amplifier (LIA) was implemented by an audio frequency ( $f \approx 300 \text{ Hz}$ ) field modulation  $\Delta H_m/4 \approx 1.6 \times 10^{-8} \text{ T}$ . The field modulation  $\Delta H_m$  corresponds to one flux quanta ( $\Phi_0$ ). The transfer function of the SQUID field detector is  $1.1 \times 10^{-10} \text{ T}/\mu\text{V}$  at the LIA. Thus from the LIA output we can calculate the field generated by the sample.

Our detection was done without any biasing dc magnetic field and we did not use a flux-locked loop. Given the small flux change seen in the experiment ( $\approx \Phi_0$ ) it was a less noisy option compared to the flux locked loop detection mode. The flux noise  $S_\phi$  of the detection circuit down to  $1 \text{ Hz}$  had a spectral power of  $10^{-6} \Phi_0^2/\text{Hz}$  which is much less than the magnetic signal detected in our experiment. The sample with the leads attached for taking the  $I$ - $V$  measurements was put on top of the tank circuit. Thus high detectability of the magnetic signal was ensured because of the close proximity of the SQUID detector with the sample, and we can detect the magnetic signal simultaneously while taking the  $I$ - $V$  data. It is the use of the high  $T_c$  SQUID that enabled us to do the experiment at an elevated temperature of  $77 \text{ K}$ . The BSCCO SQUID used by us could be used for operation up to  $100 \text{ K}$ .

In the inset of Fig. 2 we show the resistivity ( $\rho$ ) as a

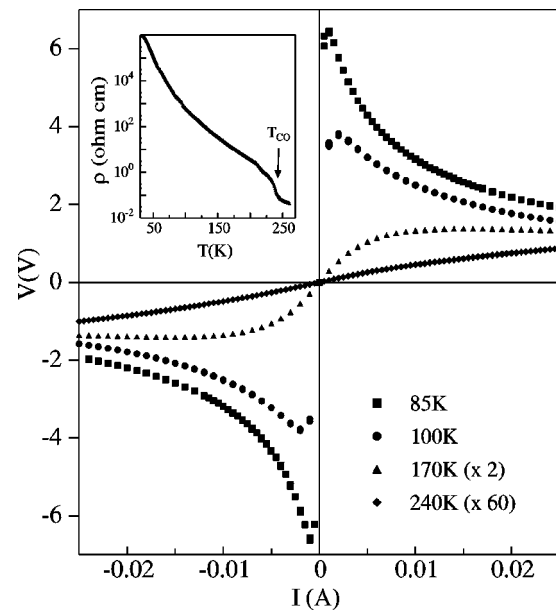


FIG. 2. The  $I$ - $V$  curves showing nonlinear conduction and negative differential resistance at different temperatures. The resistivity  $\rho$  of the sample and the charge ordering temperature  $T_{CO}$  are shown in the inset.

function of  $T$  down to  $50 \text{ K}$  measured with a very small current of less than  $0.01 \text{ mA}$  which ensures that the COI state is not destabilized. The onset of the COI state at  $T_{CO} \approx 240 \text{ K}$  can be clearly identified. The AFM order sets in at a much lower temperature, and from magnetic susceptibility measurements the  $T_N$  is found to be  $\approx 175 \text{ K}$ . The  $I$ - $V$  curves recorded at a few temperatures above and below  $T_{CO}$  show onset of nonlinear conduction at all  $T < T_{CO}$ . The nonlinearity increases as  $T$  is lowered, and below  $\approx 170 \text{ K}$  one sees the onset of negative differential resistance (NDR). The onset of the NDR regime in the  $I$ - $V$  curve and its behavior in an applied magnetic field have been the subject of a detailed investigation which is being published elsewhere.<sup>12</sup> Given the limited scope of this paper we focus only on one aspect, namely the magnetic signature of the NDR regime in the  $I$ - $V$  curve. The NDR region shows  $V \propto I^{-n}$  ( $1 > n > 0$ ). The current-induced creation of NDR is a reproducible effect and shows no change on repeated current cycling from positive to negative swing of bias current. Given the sensitivity of the experiment, any current flowing through a heater or a temperature sensor was avoided. Since the sample was in contact with the liquid nitrogen bath the sample temperature was assumed to be at  $77 \text{ K}$ . Another experiment was performed in a similar condition to measure any change of temperature that might arise due to joule heating. The temperature sensor (a  $100 \Omega$  Platinum resistance) was mounted directly on the sample and the combination was dipped in the liquid nitrogen bath. The temperature increased from  $77 \text{ K}$  by about  $0.5 \text{ K}$  at the threshold current and  $\approx 2.8 \text{ K}$  at the highest power dissipation. This confirms that the formation of NDR is not due to joule heating. Also, significant heating by the sample will make the SQUID output drop because the SQUID is in intimate thermal contact with the sample.

In Fig. 3 we show the results of SQUID measurements along with the  $I$ - $V$  curve at  $77 \text{ K}$ . The output of the LIA is plotted as a function of the current flowing through the

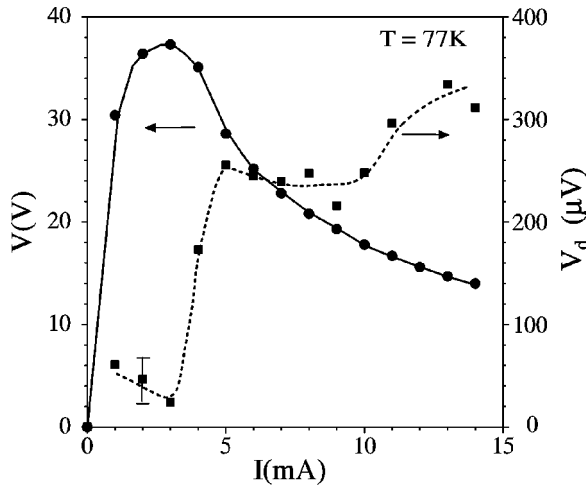


FIG. 3. The SQUID signal (output of the lock-in amplifier) at 77 K is plotted as a function of biasing current through the sample. The  $I$ - $V$  curve is measured simultaneously.

sample. This output is  $\propto$  the magnetization change ( $\delta m$ ) of the sample created by passing the current through it. Our experimental arrangement allowed us to measure the  $I$ - $V$  curve and the magnetic measurements simultaneously. We increased the bias current ( $I$ ) in 1 mA steps and covered the range up to 15 mA in  $10^4$  sec and waited for approximately 20 sec for stabilization after each current step before the lock-in reading and the voltage across the voltage leads were recorded. This method ensured that there were no effects from a changing measuring current. We find that as the sample enters the NDR regime at a current  $I \approx 3$  mA, which, assuming a uniform current density in the sample, corresponds to a current density ( $j$ ) of about  $0.5$  A/cm $^2$ , there is a clear rise in the signal from the LIA indicating a rise in the magnetization,  $\delta m$ , of the sample.  $\delta m$  increases as the current  $I$  is increased, although a jump in  $\delta m$  occurs when  $I \approx 3$  mA where the NDR regime sets in. For  $5$  mA  $< I < 10$  mA, ( $0.9 < j < 1.7$  A/cm $^2$ ), the LIA signal shows a plateau and increases further when  $I$  is increased beyond 10 mA. Our experiment thus establishes that the current-induced destabilization of the COI order leads to an enhancement of the magnetization (albeit small) indicating onset of ferromagnetic correlations.

It has been found recently, that the nonlinear conduction in the COI state is associated with a large voltage fluctuation.<sup>9</sup> We find that a large broadband noise with a power spectrum  $\sim 1/\text{frequency}$  does indeed appear in our system at the onset of nonlinear conduction. The noise power measured at 6 Hz is plotted as a function of the applied current bias  $I$  in the inset of Fig. 4. Interestingly, we find that even this fluctuation has a magnetic signature. In Fig. 4, we show the measured flux noise of the SQUID. The flux noise was measured by measuring the voltage noise of the LIA output by a spectrum analyzer. The flux noise was then calculated using the relation  $S_\phi = S_v / (\delta v / \delta \phi)^2$ , where  $S_v$  is the spectral noise power of the voltage output of the LIA and  $\delta v / \delta \phi$  is the transfer function of the SQUID. The flux noise below 1 Hz has a  $1/f$  dependence and above 1 Hz is a broad noise with superimposed peaks. At  $I = 0$  mA, the flux noise  $S_\phi(I = 0 \text{ mA}) \approx 10^{-6} \Phi_0^2/\text{Hz}$  and at  $I = 8$  mA ( $j \sim 1.4$  A/cm $^2$ ) when the  $I$ - $V$  curve is in the NDR regime,

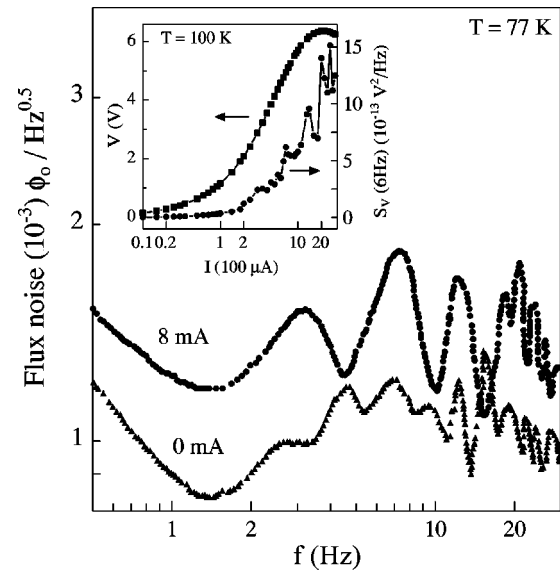


FIG. 4. Measured flux noise seen in the SQUID for  $I = 0$  and 8 mA at 77 K. The inset shows the appearance of a large broadband noise seen across the voltage probes at the onset of nonlinear conduction at 100 K.

there is a clear rise in the flux noise and  $S_\phi(I = 8 \text{ mA}) \approx 4 \times 10^{-6} \Phi_0^2/\text{Hz}$ . This extra noise is from the sample. It appears that on passage of the current when the NDR regime (likely with a metallic filament) sets in, the resulting stage has strong spin fluctuation.

The signal in the SQUID coil does not arise from the magnetic field of the current flowing through the sample. This has been directly tested by passing the same current through a dummy resistor instead of the sample. (Though the magnitude of the field produced by a direct measuring current at the SQUID is  $\approx 0.2 \mu$  T/mA, the field at the SQUID is parallel to its plane and has negligible component perpendicular to it.)

We propose a simple scenario to explain the observations. The onset of the NDR region in the  $I$ - $V$  curve beyond a certain value of  $I$  is due to the appearance of the metallic filaments which carry most of the current. This decreases the voltage across the sample. On passing more  $I$ , the volume fraction of the filament increases, leading to a further decrease of voltage, and the NDR regime is sustained. The SQUID observations show that the filaments so formed have ferromagnetically aligned Mn moments which enhance the magnetization. We may consider the filaments as made up of the FMM phase. NDR is also seen in the  $I$ - $V$  characteristics of single crystals of the same system on application of laser light. Direct observation using reflection measurements show that in this region there is formation of “metallic” filament.<sup>6</sup> Interestingly, a small jump in magnetization was also seen in laser induced melting.

The output signal at the LIA which has been directly calibrated by applying a known dc signal in a field coil can be used to estimate magnetic moments generated on the sample. The transfer function of the SQUID field detector is  $\approx 1.1 \times 10^{-10}$  T/ $\mu$ V measured at the LIA. At the highest value of sample current  $I$ , the field created by the sample is  $H_{\text{sample}} \approx 35$  nT. Knowing the approximate geometry of the detection scheme and assuming that the sample creates a dipolar

field, we can then estimate the total moment formed on the sample  $\mu_{sample} \approx 5 \times 10^{-15} \text{ Wb m} \approx 4 \times 10^{14} \mu_B$ . We make a simple assumption that this moment arises from a ferromagnetic region with all the  $\text{Mn}^{3+}$  and  $\text{Mn}^{4+}$  aligned, the estimated volume of the region will then be  $V_{fm} \approx 6 \times 10^{12} \text{ nm}^3$ . (This has been estimated from the lattice constant and saturation moment of  $3.8 \mu_B/\text{Mn ion}$ .) This is a lower limit on  $V_{fm}$ . If we assume that the magnetic moment resides on the filaments of the FMM region of volume  $V_{fm}$ , as stated before, and the filament has to span a length between the current pads ( $250 \mu\text{m}$ ) we can put a lower limit on its cross section,  $A_{fm} \approx 24 \mu\text{m}^2$ . This cross-sectional area is a tiny fraction of the total cross section, ( $A_{fm}/A_s \sim 4$

$\times 10^{-5}$ ), where  $A_s$  is the total cross section of the sample. These simple estimates are based on assumptions which are not too rigorous, nevertheless they set the scale of magnetic moment  $\mu_{sample}$  and the  $V_{fm}$  created by the application of the current. The important issue is that at the onset of NDR a small but finite magnetic moment appears on the sample.

To conclude, we find that in charge-ordered  $\text{Pr}_{0.63}\text{Ca}_{0.37}\text{MnO}_3$ , a current can destabilize the CO state giving rise to a region of negative differential resistance which sets in beyond a current threshold. The appearance of the NDR region gives rise to a small increase in the magnetization suggesting that the NDR region arises from filaments of the FMM phase formed by the current.

<sup>1</sup>H. Kuwahara, Y. Tomioka, A. Asamitsu, Y. Moritomo, and Y. Tokura, *Science* **270**, 961 (1995).

<sup>2</sup>*Colossal Magnetoresistance, Charge Ordering and Related Properties of Manganese Oxides*, edited by C.N.R. Rao and B. Raveau (World Scientific, Singapore, 1998).

<sup>3</sup>A. Asamitsu, Y. Tomioka, H. Kuwahara, and Y. Tokura, *Nature (London)* **388**, 50 (1997).

<sup>4</sup>C.N.R. Rao, A.R. Raju, V. Ponnambalam, Sachin Parashar, and N. Kumar, *Phys. Rev. B* **61**, 594 (2000).

<sup>5</sup>K. Ogawa, W. Wei, K. Miyano, T. Tomiyoka, and Y. Tokura, *Phys. Rev. B* **57**, R15 033 (1998).

<sup>6</sup>M. Fiebig, K. Miyano, Y. Tomiyoka, and Y. Tokura, *Science* **280**, 1925 (1998).

<sup>7</sup>Y. Okimoto, Y. Tomioka, Y. Onose, Y. Otsuka, and Y. Tokura, *Phys. Rev. B* **57**, R9377 (1998).

<sup>8</sup>A. Biswas, A. Arulraj, A.K. Raychaudhuri, and C.N.R. Rao, *J. Phys.: Condens. Matter* **12**, L101 (2000).

<sup>9</sup>A. Guha, A. Ghosh, A.K. Raychaudhuri, S. Parashar, A.R. Raju, and C.N.R. Rao, *Appl. Phys. Lett.* **75**, 3381 (1999).

<sup>10</sup>R. Kajimoto, T. Kakeshita, Y. Oohara, H. Yoshizawa, Y. Tomioka, and Y. Tokura, *Phys. Rev. B* **58**, R11 837 (1998).

<sup>11</sup>S. Chaudhury, N. Khare, A.K. Gupta, and V.S. Tomar, *J. Appl. Phys.* **72**, 1172 (1992).

<sup>12</sup>Ayan Guha, A.K. Raychaudhuri, A.R. Raju, and C.N.R. Rao, *Phys. Rev. B* **62**, 5320 (2000).